Journal of Seismology (2005) **9:** 449–462

Effect of lateral variation and model parameterization on surface wave dispersion inversion to estimate the average shallow structure in the Paraná Basin

Meijian An[1,2] & Marcelo S. Assumpção[1,*]
[1]*Department of Geophysics, IAG, University of São Paulo, Rua do Matão 1226, São Paulo, SP, 05508-090, Brazil;* [2]*Now at Lab. Computational Geodynamics, the Graduate University of Chinese Academy Sciences, Beijing, China;* [*]*Author for correspondence: e-mail: marcelo@iag.usp.br*

Received 29 July 2004; accepted 5 September 2005

Key words: Brazil, heterogeneous structure, genetic algorithm, surface wave dispersion inversion

Abstract

The average layered structure of the intracratonic Paraná Basin, SE Brazil, is investigated with surface-wave group velocities from a small regional earthquake recorded by two broadband stations. Rayleigh and Love waves in the period range 1–4.2 s are used to infer average properties down to about 4 km. Genetic algorithm techniques are used to find the best fitting 1-D S-wave model. The inverted 1-D models show fair correlation with the average properties of the propagation paths as expected from geology and borehole information. However, different S-wave velocity models are obtained for the different inversion parameterizations. Since lateral heterogeneities are expected along the paths, several synthetic tests are performed with heterogeneous propagation paths. For approximately homogenous path (i.e., little lateral variation), the main features of the average synthetic model can be retrieved for different model parameterizations. For strong lateral variations, however, the average dispersion curve can produce very different 1-D inverted models depending on the parameterization. Also, the 1-D inverted models may differ significantly from the average properties of the inhomogeneous path, and wrong depths to interfaces may be inferred. For real data inversions, it is then suggested that various different parameterizations should be tested. If the resulting models show consistent features, this probably indicates homogeneity in the propagation path. But, if very different and unstable features are obtained in the 1-D inversions, then strong lateral variation may be present in the propagation path, and the average 1-D model may not represent average properties along the path.

Introduction

Surface wave dispersion is extensively used to get the S-wave velocity structure in many different depth scales. In seismology, long-period surface waves (up to 200 s) are used to study the upper mantle structure down to about 300 km depth. Short-period surface waves (∼0.5 to 2 s) can give information on the shallow crustal layers, such as sediments, down to a few kilometers (e.g., Kocaoglu and Long, 1993; Chourak et al., 2001). In seismic exploration, high frequency Rayleigh waves can be used in geotechnical studies of soil down to tens or hundreds of meters as if it were an *in-situ* method to determine shear-wave velocity profile (Stokoe and Nazarian, 1983; Stokoe et al., 1989).

Surface wave dispersion is commonly inverted with linearized least squares techniques such as in estimating the crustal and upper mantle structure (e.g., Herrmann, 1987; Herrmann and Ammon, 2002) or in geotechnical studies (e.g. Stokoe and Nazarian, 1983). In recent years, global algorithms have been applied to the inversion of surface wave dispersion, such as Genetic Algorithm (GA) (Lomax and Snieder, 1995; Shi and Jin, 1996; Yamanaka and Ishida, 1996; Zhang et al., 1998; An and Assumpção, 2001, 2005) and Neighborhood Algorithm (NA) (Snoke and Sambridge,

2002). Lomax and Snieder (1995) configured the simple GA (SGA) parameters and misfit function to search all acceptable models. Zhang et al. (1998) compared the acceptable results of SGA inversion with those of linearized least squares, and concluded that SGA can be used to map out the model space. In these experiences, SGA is used to sample all acceptable models but not to find the best model. In order to get the best result, Shi and Jin (1996) analyzed manually the distribution of all model parameters, and showed that SGA can find the best model in the inversion of surface wave dispersion. Using all previous optimal models to constrain the parameter space to smaller ranges often improves the total search efficiency (An and Shi, 1996). Yamanaka and Ishida (1996) applied SGA to the inversion of a shallow structure (4 to 15 km) using surface wave dispersion (1–20 s). An and Assumpção (2005) combined genetic algorithm with a random trial and error jump ("hybridized" GA) to further improve the good models in each generation. Because this hybridized GA (HGA) not only is less sensitive to the initial models, population size and the search resolution but also can find the optimum solution and explore wide acceptable model space (An and Assumpção, 2005), it is used in this paper.

Inversion of surface wave dispersion is usually done with horizontally homogeneous model. In real observations, the path always crosses different geological provinces, and the resulting 1-D model is taken to represent an average of the structure along the path. But how similar to the "average" structure is the inverted model? This is an important question in interpreting the inverted models. Kennett and Yoshizawa (2002) showed the horizontal strongly heterogeneous path can cause obvious perturbation on the observed phase (velocity) of surface wave because the trajectory is controlled by the phase-speed variations. If the variation on the trajectory is considered, can the path-average model represent the average structure? In this paper, we used synthetic tests to study the effect of lateral variations on the inverted 1-D path-average model and how to identify the strong horizontal heterogeneity from inverted models, which can help the interpretation of the real data.

The intracratonic Paraná Basin has been studied with long-period (10–150 s) surface waves by Snoke and James (1997), Zhang et al. (1998), Snoke and Sambridge (2002), and An and Assumpção (2001, 2005). The estimated lithospheric thickness is at least 100 km. Crustal thicknesses varies from 40 km, near the edges, to about 47 km near the center of the Paraná Basin, as determined from receiver functions (Assumpção et al., 2002). Thicker crust occurs approximately where total sediment is also thicker (about 6 km). The observed long-period surface waves have no resolution on the sedimentary (0–5 km) layers. Because of the strong trade-off between all parameters in the surface wave inversion, the lack of constraints on the sedimentary layers increases the uncertainty in the estimated upper crustal S-wave velocities. Average velocities in the sediments could better constrain the crustal models in studies with long-period surface waves. Here we use group velocities of short-period (1–4.2 s) surface waves from one small earthquake (magnitude 3.8 m_b) to study the average properties of the sedimentary layers. Seismic activity in the Paraná Basin is one of the lowest in Brazil (Assumpção et al., 1997), and this event presents a rare chance to study the basin's average structure with surface wave dispersion.

Study region and observed data

The intracratonic Paraná Basin in SE Brazil started subsidence in the Early Paleozoic and had three main depositional sequences in the Paleozoic predominated by sandstones (Silurian, Devonian and Permo-Carboniferous). During the Mesozoic, the basin evolved with deposition of two major continental sedimentary sequences: Triassic Piramboia Formation, and Jurassic Botucatu Formation (Zalán et al., 1988, 1990). In Early Cretaceous (~137–130 Ma), just prior to the South Atlantic opening, a large volume of basalt flow covered the entire basin reaching thicknesses up to 1.5 km (Serra Geral Formation) near station POPB (Figure 1). After the Atlantic rift, additional subsidence allowed another sequence of sandstones (Bauru Formation) making the total thickness of the Paraná Basin reach more than 6 km in some places (Melfi et al., 1988; Zalán et al., 1990).

The simplified geological map in Figure 1a shows the epicenter of a local earthquake (Sept. 28, 2000, magnitude 3.8 m_b) and two broadband stations (POPB and CANB). In the study region, the superficial post-volcanic Bauru formation is very thin and variable, less than 200 m or so. Besides this thin surface layer, there are three main layers: (1) Serra Geral basalt varying from a few hundred meters to about 500 m for CANB path and 680–1500 m for POPB path (Melfi et al., 1988); (2) pre-volcanic sediments, about 1.6–2.2 km thick for CANB path and 1.6–3.5 km for POPB path (Melfi et al., 1988); and (3) granitic/gneissic basement. The geological profile shows stronger thickness

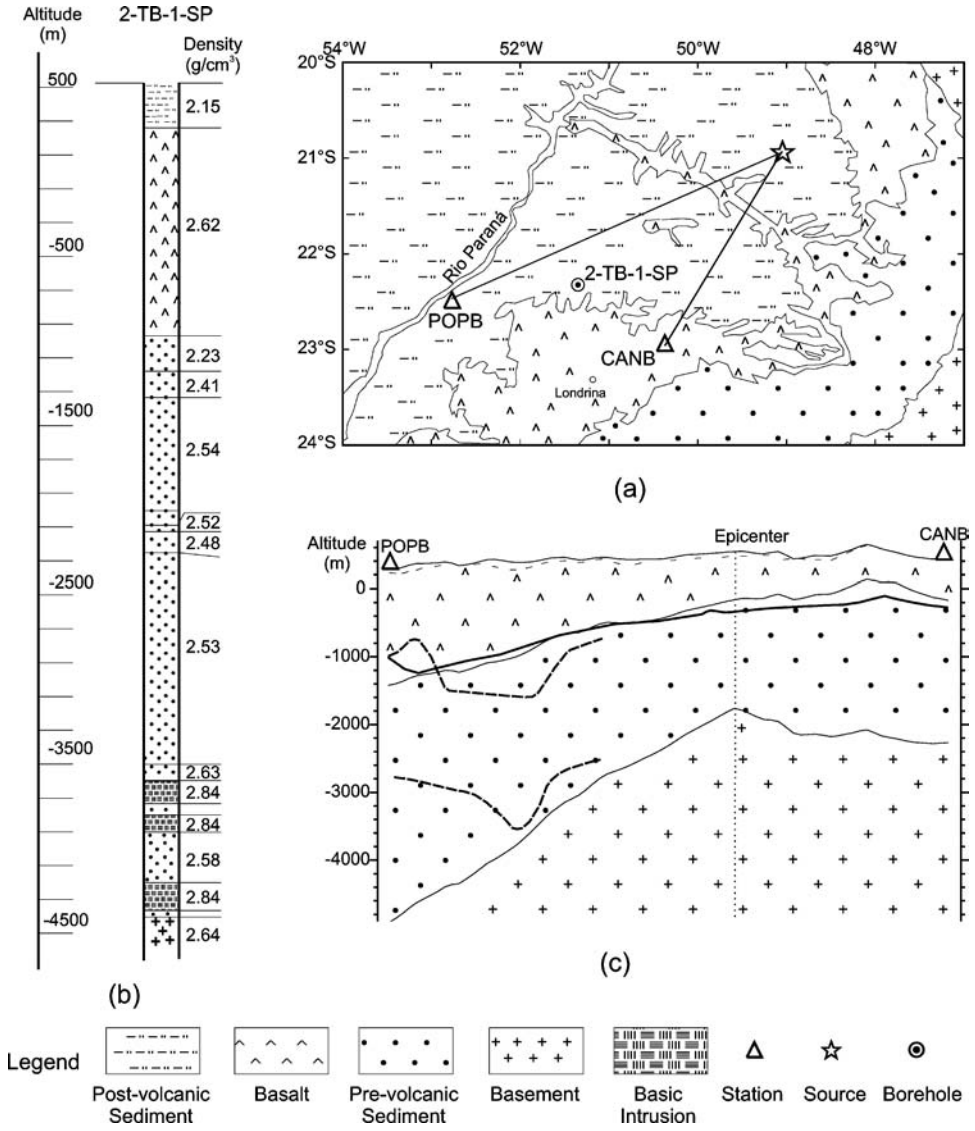

Figure 1. (a) Geological (Schobbenhaus and Bellizzia, 2000) and geographical information. (b) Data from borehole 2-TB-1-SP (CESP, 1991) whose position is shown in (a); note low densities just below the basalt. (c) Simplified profile along ray paths. Topography is from ETOPO5. Thin dashed line is the bottom boundary of post-volcanic sediments (Melfi et al., 1988); interface in thin solid lines are from Melfi et al. (1988), in thick solid lines from DAEE (1976, 1979), in thick dashed lines are estimated from MT surveys (Stanley et al., 1985).

variations in the POPB path compared to the CANB path. Uncertainties are obvious in the depth mapping of these interfaces as seen in Figure 1c. Borehole data (Figure 1b) shows very low densities of pre-volcanic sediments just below the basalt layer, indicating that a large velocity contrast should be expected at the base of the basalt layer. Also, some basic sills in the bottom of the pre-volcanic sequence can be observed.

Figures 2a–d show the original seismograms, instrument corrected and band-pass filtered at 1–5 s, together with the result of the phase-matched filter used to isolate the fundamental mode for each type of wave. Preliminary surface wave group velocities were determined by multi-filtering technique (Dziewonski et al., 1969; Herrmann, 1987; Bhattacharya, 1983) using instrument-corrected traces such as in Figure 2e. These initial velocities were then used to isolate the fundamental mode using phase-matched filter (Herrin and Goforth, 1977; Herrmann, 1987; Levshin et al., 1998). All observed fundamental-mode group velocities of

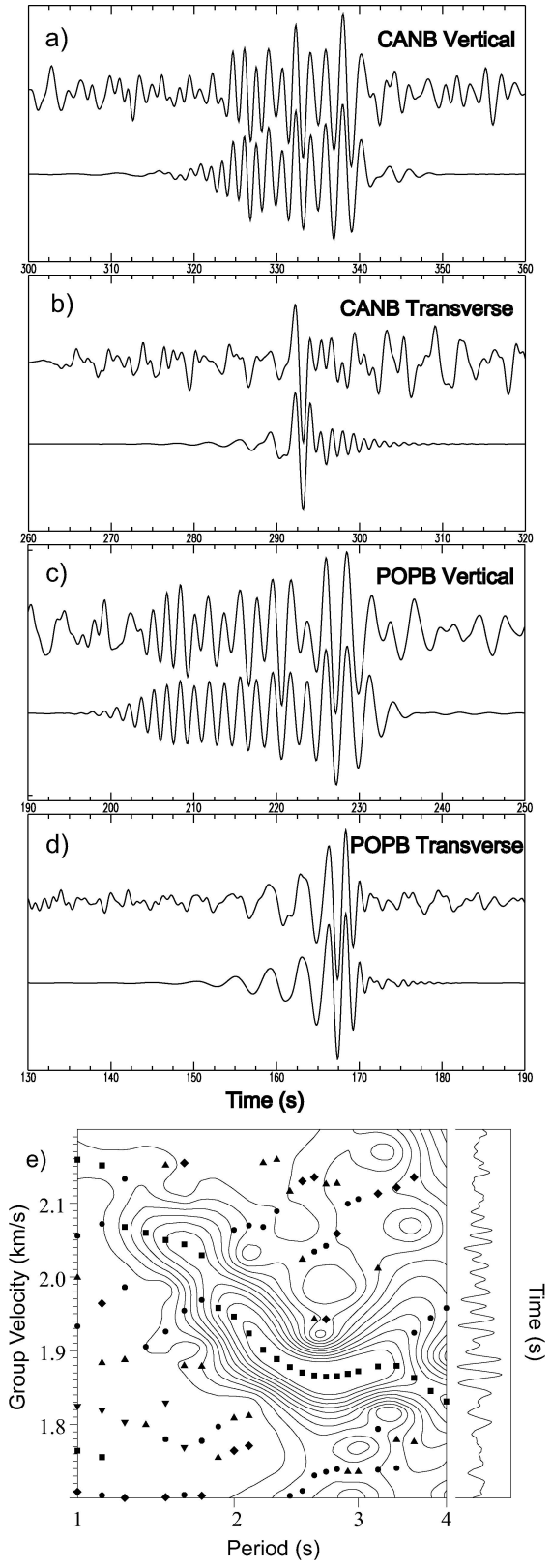

Rayleigh and Love waves (Figure 4) were determined by multi-filtering technique using the phase-match-filtered traces. The seismological programs V3.15 of Herrmann (2001) and Herrmann and Ammon (2002) were used. Because uncertainties in group velocities are difficult to be determined when only one event is available, uncertainties of one period for the arrival time of the envelope peaks are taken as the observation errors (bars in Figure 4).

The largest observed periods are about 3.3 s for CANB and 4.2 s for POPB, which correspond to wavelengths of about 8 km and 11 km, respectively. The fundamental mode surface wave has good constraint on the S-wave velocities above a depth of about one-third of its wavelength. This means the observed data can be inverted for well constrained S-wave structure down to about 3 km depth for CANB and about 4 km for POPB.

Model parameterization

We used 1-D models with plane layers characterized by: S-wave velocity (β), P-wave velocity (α), density (ρ) and thickness (h). The sensitivity of the surface wave dispersion to each parameter is different and depends on the structure itself, because of the non-linear nature of the surface waves. It is well known that S-wave velocity is the most significant parameter in surface wave dispersion inversion with P-wave velocity and density having only a small effect. For this reason, it is seldom possible to invert for all parameters independently. In this paper, we use a fixed P- to S-velocity ratio (α/β) of 1.732 and calculate the density from the P-wave velocity.

The inversion was done in three modes with different model parameterizations:

Mode 1: S-wave velocity and thickness of a small number of layers. We invert for both S-wave and thickness of three layers above a half-space trying to get the main features of our model, that is, one basaltic layer, two layers of pre-volcanic sediments and the basement. This modeling was based on the geological information (Figure 1).

Figure 2. (a) Vertical and (b) transverse components of the event (Sept. 28, 2000) recorded at stations CANB; (c) and (d) at POPB. Each diagram shows the instrument corrected displacement, band-pass filtered at 1–5 s, on top; and the phase-match-filtered trace below. (e) Contour of envelope amplitudes from multiple filtering of POPB Rayleigh waves (top trace in c); symbols show largest and secondary amplitude peaks.

Mode 2: Multi-layer, with fixed thicknesses. We use five layers for the basin sequences with fixed thicknesses (four first layers with 0.5 km, and the fifth layer with 1.0 km), and a half-space. Only S-waves are inverted for.

Mode 3: Smoothed multi-layer mode. This mode is the same as the previous mode, but with additional constraint of S velocity smoothness between layers.

Although smoothing is often necessary to avoid instabilities in the inversion, it is helpful to carry out an inversion without smoothing to study the origin of such instabilities before interpreting the results.

To invert the observed dispersion curves, we used HGA (An and Assumpção, 2005). Ten more initial search loops are used to collect good ("optimized") models (An and Shi, 1996; An and Assumpção, 2004). The search ranges are reduced, based on those optimized models, and the algorithm then continues with the new optimized ranges. The forward model was computed with the code *surfmo* (Lomax and Snieder, 1995). GA parameters were: population size 32; mutation probability 0.02; cross-over probability 0.85; string length 12 for all parameters. In each generation, other ∼15 models will be evaluated in the local trial and error iteration of HGA. All good/acceptable evaluated models are saved. In the inversion mode 1, with S-wave and thickness, the total model space was $2^{12\times7} \approx 1.9 \times 10^{25}$. The maximum generation is set when the best model stops optimizing significantly.

The minimized objective function, the misfit of the group velocities Q_u, is a modified *rms* difference between calculated and observed group velocities (equation (1)). n is the total number of observations, U_i^o and U_i^c are the ith observed and calculated group velocities, σ_i is the observation error of U_i^o, and the penalty P_i is zero unless $|U_i^o - U_i^c| > \sigma_i$. In that case, $P_i = (|U_i^o - U_i^c|^2/\sigma_i^2 - 1)$. The penalty P_i forces the models' dispersion to stay within the uncertainty limits.

$$Q_u = \sqrt{\frac{\sum_{i=1}^{n}\left[\frac{(U_i^o-U_i^c)^2}{\sigma_i^2} + 4P_i\right]}{\sum_{i=1}^{n}\left(1/\sigma_i^2\right)}} \qquad (1)$$

Penalty terms are sometimes included in the cost function in random global optimization algorithms, such as used by Snoke and Sambridge (2002) with Neighbourhood Algorithm.

In the inversion mode 3, another objective, smoothness $Q_{\text{smooth}}(=\Sigma|Vs^j - Vs^{j-1}|/m,\ j = 2, m)$, can be optimized simultaneously in the inversion process. This is a simple multi-objective inversion problem. Usually all objective functions are integrated into a single objective function in the optimization. We used the sum of weighted objectives to be minimized: $Q = Q_u + w \times Q_{\text{smooth}}$, where w is the smoothness weight (0.01–0.1).

The search ranges (thickness, S-wave velocity) of all layers used in the inversion mode 1 are respectively from the surface to the bottom: (0.1–1.5 km, 1.0–3.5 km/s), (0.1–3.0 km, 1.0–3.5 km/s), (0.1–4.0 km, 1.5–4.0 km/s), (half-space, 1.5–4.0 km/s). For the fixed thickness inversions, modes 2 and 3, the S-wave range was set to 1.5 to 4.0 km/s for all layers.

Inversion of observed data

Station CANB

Figures 3a, c, e show the good inverted models for station CANB using the three inversion modes respectively. Figures 4a, c, e show their fitness. When inverting for both S velocity and thickness (Figure 3a), a thin low-velocity layer, the 2nd layer from depth 0.5 km to 0.8 km, corresponds well to the lowest densities just beneath the basalt layer in the borehole log (Figure 1). The two low-velocity layers together, the 2nd and 3rd layers from about 0.5 to 3 km, correspond to the pre-volcanic sediments (Figure 1). The top of the basement is modeled at 3.2 km depth in good agreement with the expected average depth of 2.6 km from Figure 1. In the multi-layer inversion mode 2 (Figure 3c), strong variations in the S-wave can be seen in the 2nd and 3rd layers. Below 1.5 km depth, the S-wave velocities are similar to those of inversion mode 1. The smoothed multi-layer inversion mode (Figure 3e) shows the same general trend of modes 1 and 2. Note that the misfit of the best models are similar for modes 1 and 2 (0.003 and 0.004 km/s, respectively), whereas the smoothness constraint in mode 3 increases the group velocity misfit (Q_u) of the best model to about 0.012 km/s.

The models in the three inversion modes for CANB show the same main features, that is, a high velocity surface layer (basalt) about 0.5 km thick, a low velocity sequence (pre-volcanic sediments), and high velocities for the basement below about 3 km depth. This inverted S-wave layered structure is in good agreement with the expected geological structure shown in Figure 1. The basement velocity also agrees with the average Paraná Basin upper crust (3.67 km/s) obtained by Snoke and James (1997).

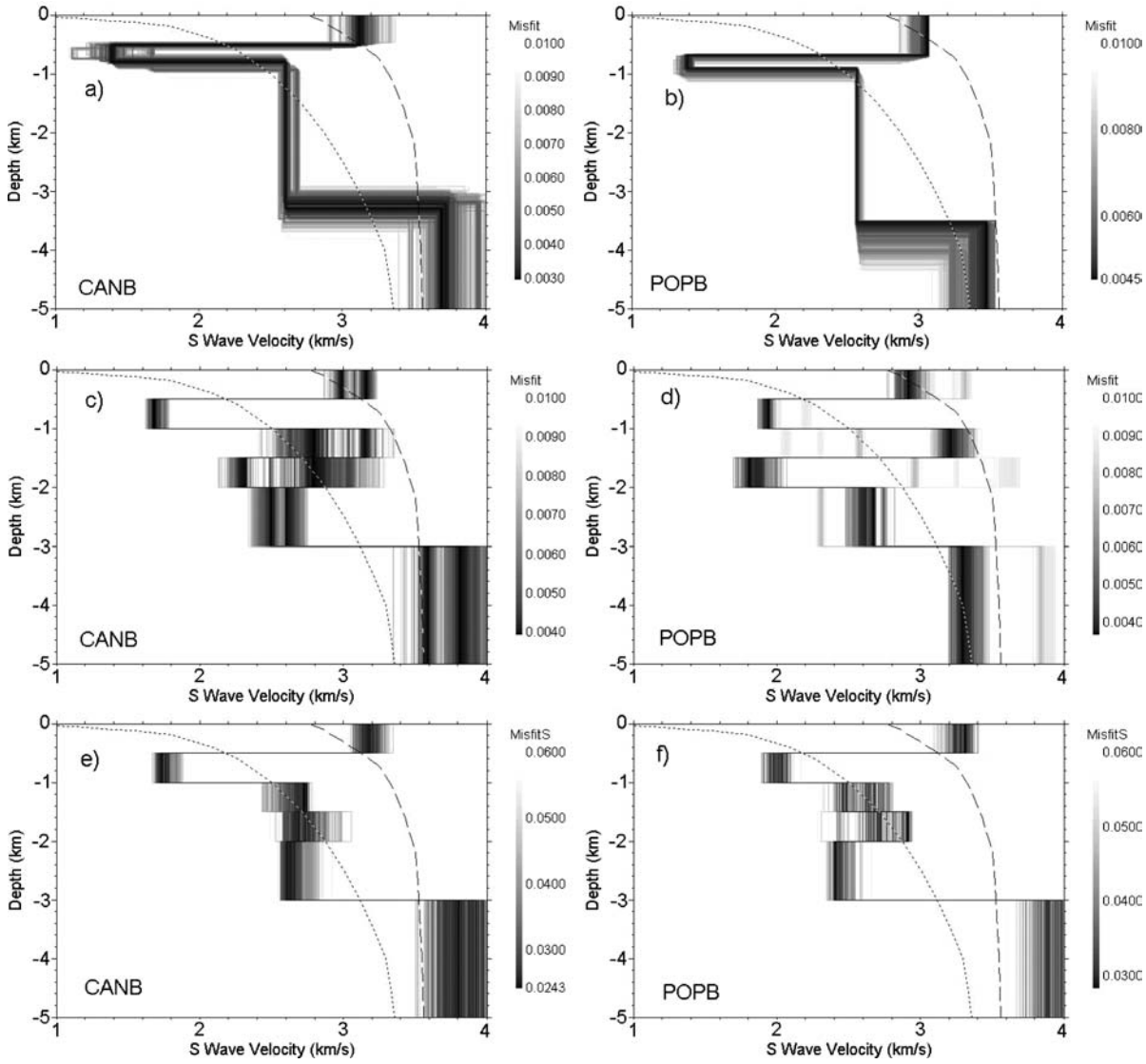

Figure 3. The good inverted models in grayscale of misfit (Q_u) or misfitS ($Q_u + 0.01Q_{\text{smooth}}$). (a) and (b) inversion mode 1 with both S-wave and thickness inverted. (c) and (d) inversion mode 2. (e) and (f) inversion mode 3; all displayed models have smoothness $Q_{\text{smooth}} < 1.2$ km/s. The dots and the dashes are the average velocity profile of generic rocks and of the very hard generic rocks in eastern North America (Boore and Joyner, 1997) respectively. Misfit or misfitS in all diagrams are in km/s.

Station POPB

Figures 3b, d and f shows that the good inverted models for station POPB have about the same general features seen in the CANB models. When inverting for both S-wave and thickness (Figure 3b) the first layer is thicker and the second layer, the low-velocity layer, is narrower than that of CANB. The inversion mode 1 indicates not only that the first high velocity layer (basalt) is thicker along the POPB path compared with CANB, as expected, but also a basement depth of 3.5–3.6 km in good agreement with the average depth expected from Figure 1 (3.4–3.8 km). The basement (half-space) velocities for POPB are lower than those of CANB; but still near the range expected for the upper crust in shield/platform areas (Christensen and Mooney, 1995), and between the generic rocks and very hard generic rocks (Boore and Joyner, 1997). In the inversion mode 2

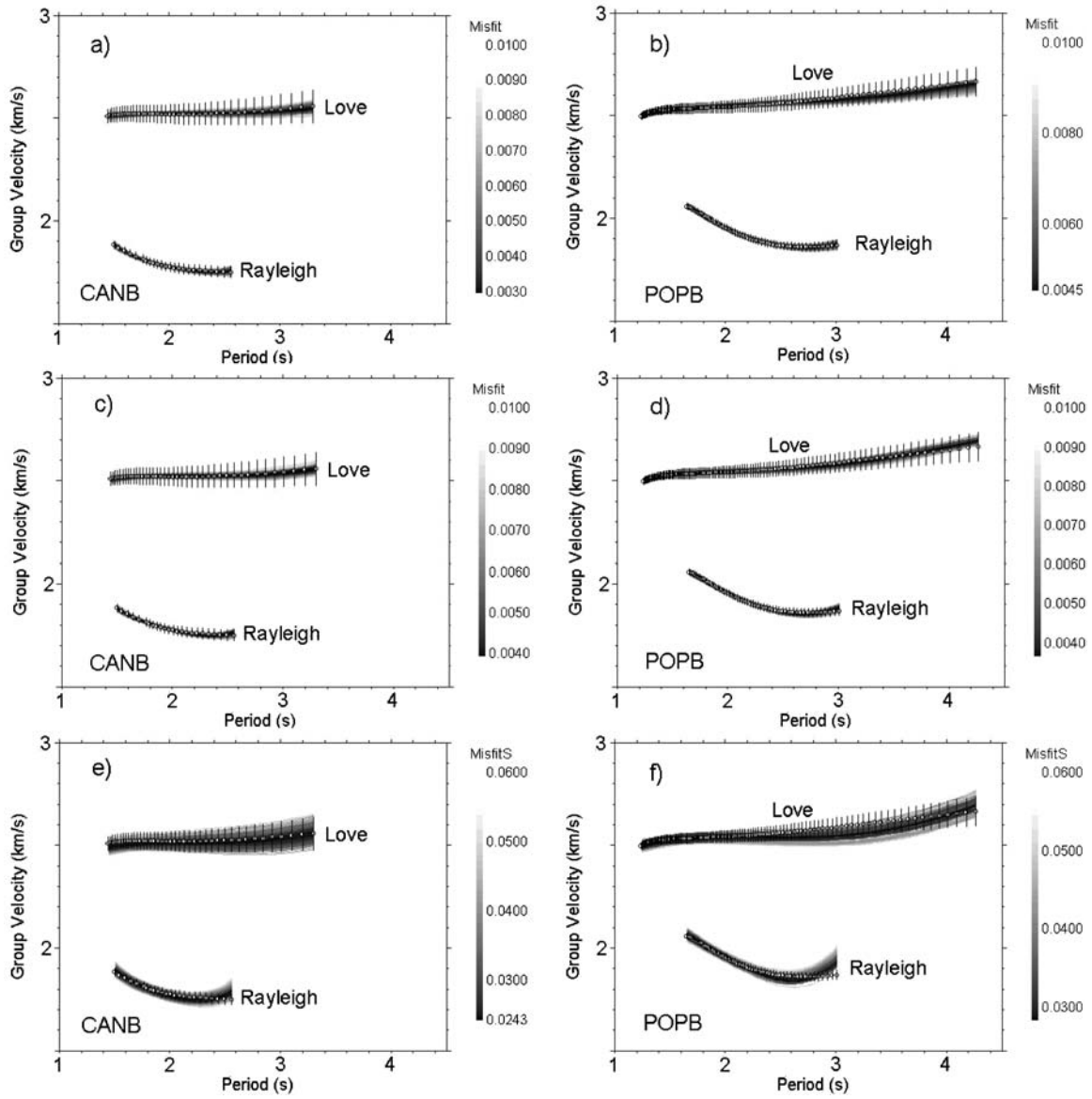

Figure 4. The fitness of models in Figure 3. The dots with error bars are the observed group velocities.

(Figure 3d), the S velocity oscillations from second to fourth layers are stronger indicating higher instabilities, compared to CANB.

The models obtained in the inversions above show general similarities to the expected geological data. But in the unsmoothed, fixed thickness inversion mode, there appear some abnormal layers alternating very high and very low velocities in POPB path. Is this effect just inversion instability due to errors in the observation? Or could it be an effect of lateral variation of structure along the path? The structure of the sedimentary basin varies along the seismic path, especially for POPB (Figure 1). On the other hand, it is usually assumed that a 1-D model shows the average properties of a laterally varying structure. While this may be a valid assumption for paths with "weak" heterogeneities, it is seldom seen in the literature any tests of how much lateral variation is allowed before the 1-D model is no longer useful, and what "average" inverse results would appear for the "strong" horizontal inhomogeneous path. Here, we will investigate the effect in fitting a 1-D model to an observed

dispersion curve that sampled the path with lateral variation.

Synthetic tests for lateral variation

First of all, we tested the capability of our HGA to find the synthetic solution (Figure 5) by inverting a three-layer structure. In this test we fixed the basement velocity, as done in the other synthetic tests below, and inverted for both S-wave and thickness of three layers. The S-wave velocity of the half-space (basement) is fixed because we want to focus on the effect of lateral variation in the sedimentary layers only. The GA parameters are similar to the previous inversion with real data. All good models are shown in Figure 5a in different color shades and the synthetic model is shown by dashed line, the fitness of models is in Figure 5b. In Figure 5a, the models with misfit less than 0.002 km/s are nearly equal to the theoretical structure. So our HGA can find the theoretical model. In order to check the effect of noises in observation data, some random noises were added to the synthetic data and the results are in Figures 5c, d. The models in Figure 5c with misfit near 0.0176 km/s are nearly equal to the theoretical structure showing that random noise does not strongly influence the inversion for the best model provided the number of data points is large enough. In other inversions, random noises will not be added to the synthetic data.

Sedimentary layers can have a complex velocity profile, even within the same geological formation, as suggested by the density log of Figure 1b. For this reason we also tested if the main trend of a more complex velocity profile can be retrieved in the inversion mode 1, with a few layers. We used the theoretical dispersion curve of a six-layer sedimentary sequence over a half-space with fixed S-wave velocity of 4.0 km/s. The inversion using only three layers (Figure 5e) retrieved the main trend of the six-layer S-wave profile with the three interfaces near the depths of the larger discontinuities.

We now carried out tests to study the effect of variable layer thicknesses along the path, as expected from

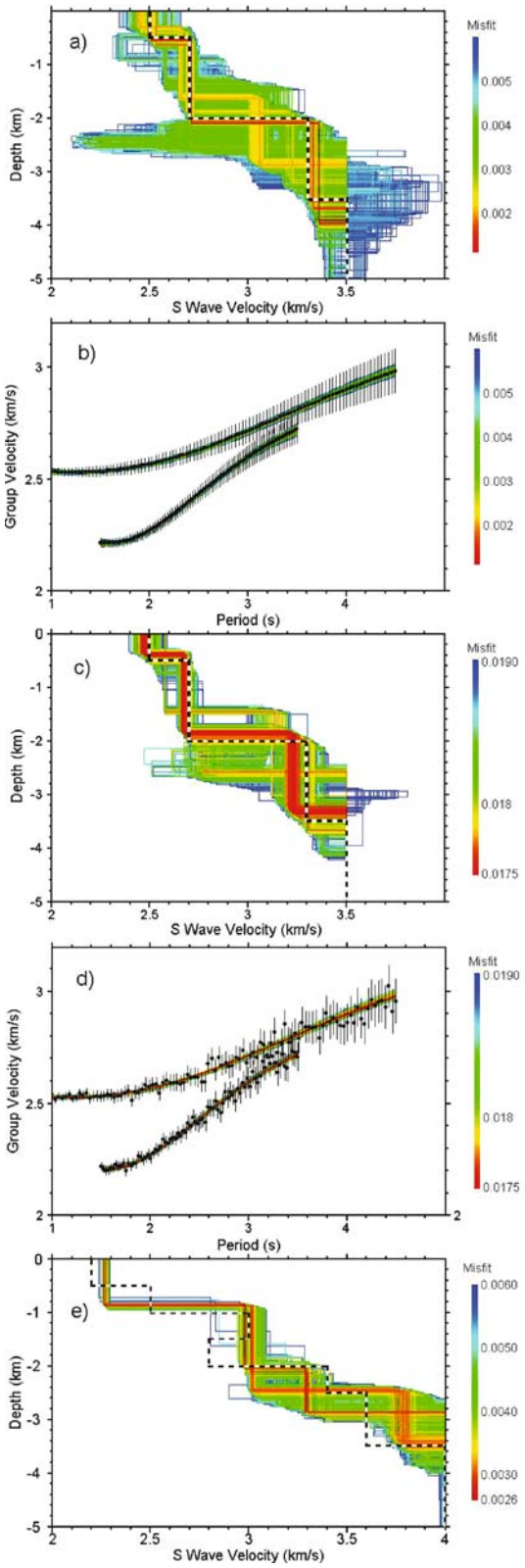

Figure 5. (a) Good models of a synthetic inversion test; the dashed line is the synthetic profile; inverted models are solid lines in color shades of misfit. (b) Group velocity fit of good models in (a). Dots with error bars are synthetic data; lines are the dispersion of good models in color shades of misfit. (c) and (d) are the same as (a) and (b) with added normal random errors. (e) Inversion with a simplified three-layer model of data from six-layer model.

Figure 1. The main purpose of these synthetic tests is to see how much the average 1D model obtained from the path-average dispersion resembles the average structure. The shallow structure in the Paraná Basin is not expected to have strong, short-wavelength lateral heterogeneities. The basement depth varies from about 2 km near the epicenter to a maximum depth of about 5 km near station POPB, 420 km away (Figure 1). The surface wave periods we use correspond to wavelengths of ∼10 km or less. Over a short path, comparable to our wavelengths, layer thicknesses should vary by less than 2%. So we are dealing with really very weakly heterogeneous structures, and strong 2D effects, such as mode conversions, should not be important. Phase and group velocities should vary smoothly along the propagation path according to the local structure. We simulated the average surface wave slowness of the composed total path as the average slowness of two homogeneous sections. Because of the smoothly varying nature of the structure, we believe the synthetic dispersion obtained by two 1D models (each one representing the average properties of each half) should give an approximation to the total dispersion good enough for our tests.

The two homogeneous sections differ in only one or two parameters. The same period ranges of the observed surface waves were used. Using these synthetic group velocities, the good models are searched and compared with the two original homogeneous sections.

Inverting for velocity and thickness (mode 1)

We designed three groups of the homogeneous section pairs, shown in Figures 6–8: (1) the two synthetic sections differ only in the S velocity of the second layer (Figure 6); (2) difference in the thickness of the first and second layers (Figure 7); (3) difference in both thickness and S-wave velocity in the second layer (Figure 8).

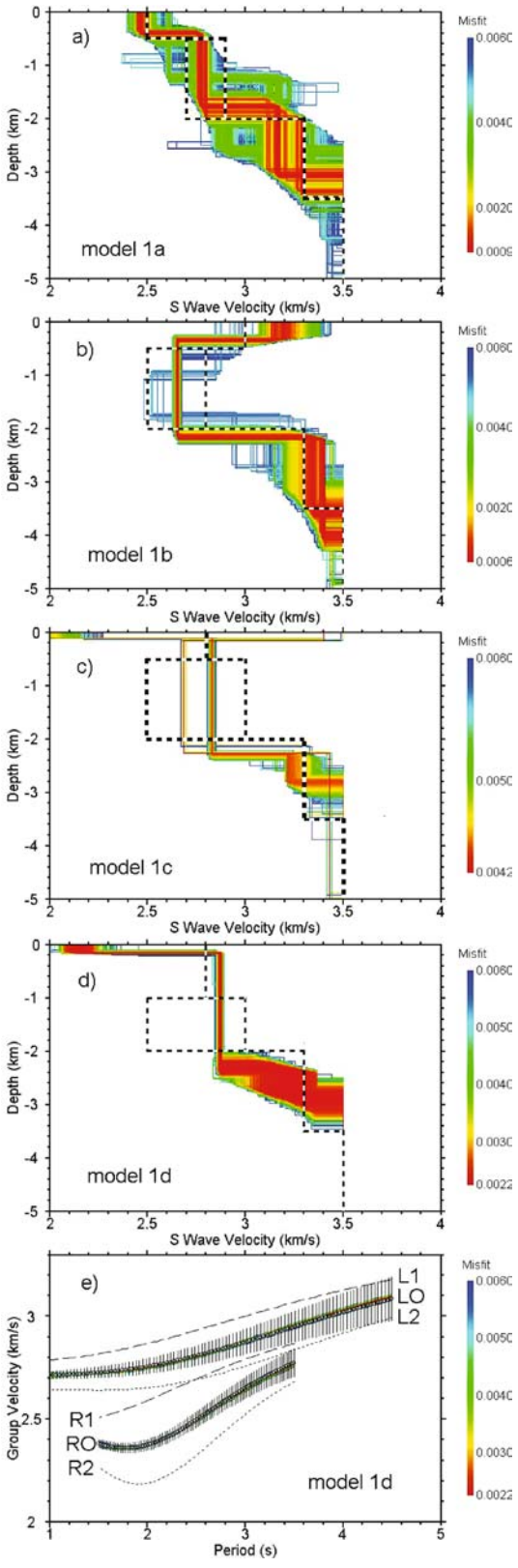

Figure 6. (a)–(d) The good inverted models of group 1 (S-wave velocity variation in the second layer) in the inversion mode 1. Two dashed lines are the homogenous sections of the synthetic profile. Inverted models are solid lines in color shades of misfit. (e) The fitness of the good inverted models in (d); dots and dashes are the group velocities of each homogeneous section; the dots with error bars are the synthetic data (average slowness) of inhomogeneous sections; lines are the surface wave dispersion of good inverted models in color shades of misfit. L1 and R1 are the Love and Rayleigh velocities of the first homogeneous section of the profile; L2 and R2 are the velocities of the other section; LO and RO are the synthetic average dispersion of the total inhomogeneous profile.

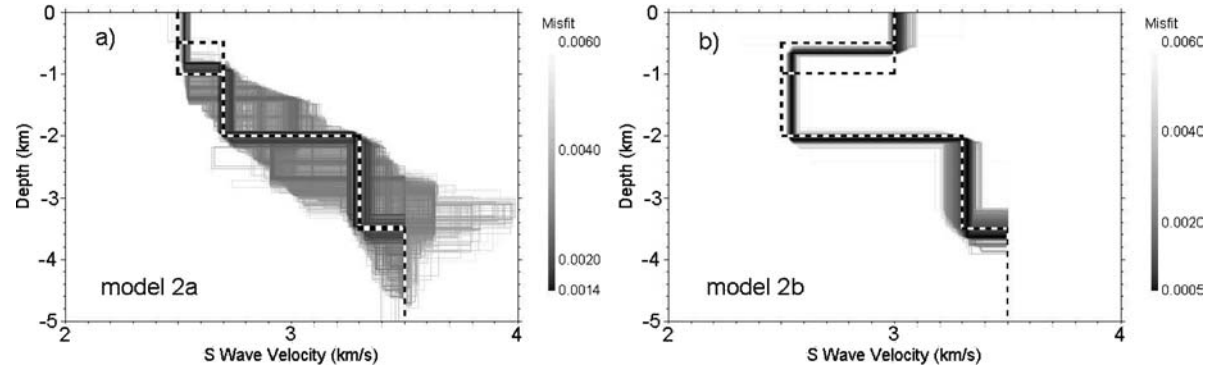

Figure 7. The good inverted models of group 2 (thickness variation in the first and second layers) in the inversion mode 1.

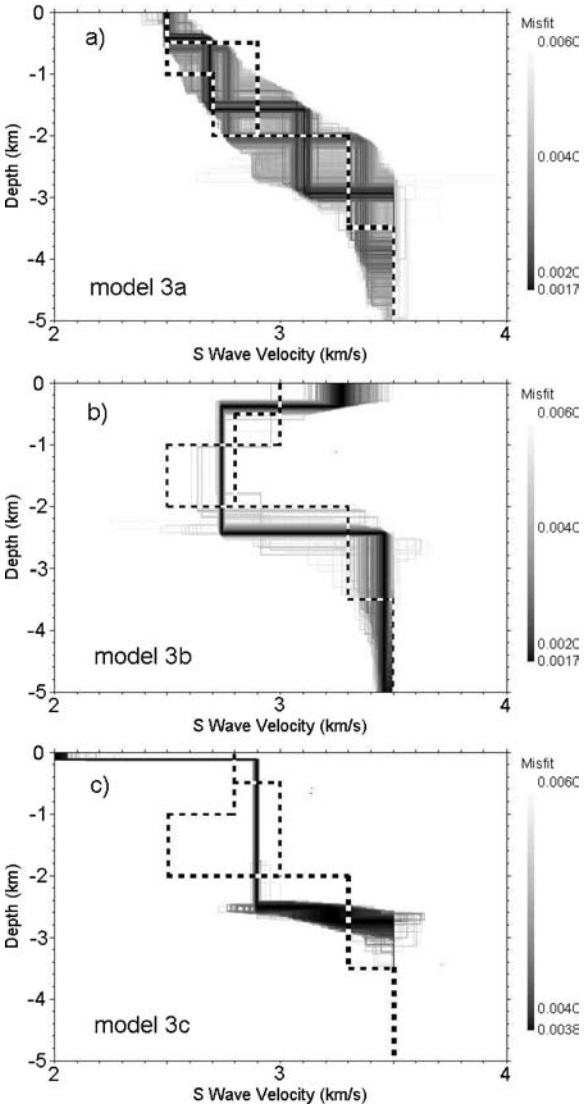

Figure 8. The good inverted models of group 3 (thickness and S velocity variation in the first and second layers) in the inversion mode 1.

In group 1 (models 1a and 1b in Figures 6a, b) a small variation of S velocity in the second layer produces the best 1-D models looking like the average profile of the two homogeneous sections. In this case, the inverted model shows the approximate average properties of the inhomogeneous profile, both for the low-velocity case and for the depth-increasing velocity profile. For model 1c (Figure 6c) where the S-wave velocity has a large difference between each homogeneous section, the thicknesses of the two first layers in the inverted model are different than any of the homogeneous section. We also tested a large difference in the second layer with a thicker first layer (model 1d, Figure 6d). The inverted model in Figures 6c, d cannot show the correct boundary between the first two layers; an artificial thin layer appeared at the surface with low or high velocity; and the estimated basement depth would be highly underestimated. Figure 6e shows the group velocities of each homogeneous section for the test models 1d, together with the composed dispersion fitness.

For group 2 (Figure 7), where the thicknesses of the first and second layers are different, the inverted models are similar to the average profile giving an intermediate thickness for the first layer. The estimated basement depth is not much affected by the heterogeneity in the first layer.

In group 3 we varied both thickness and S velocity of the first two layers (Figure 8). In models 3a and 3b, none of the major discontinuities were correctly estimated, but the S-wave velocity trends are retrieved. In case 3c, where homogeneous sections with and without low-velocity zones were combined (Figure 8c), the inversion resulted in a thicker second layer with a thin low-velocity surface layer.

These tests show that the inverted 1-D model most differs from the average of the two homogeneous

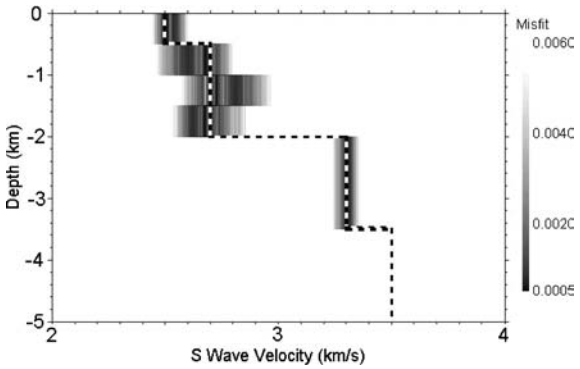

Figure 9. The good inverted models of a synthetic test in the inversion mode 2 to check the convergence of the HGA algorithm.

sections when there is a large lateral variation (cases 1c, 1d, 3a, 3b and 3c), specially when one section has a low-velocity zone, and the other does not, such as cases 1c, 1d, 3c. If the lateral variation is small (cases 1a, 1b) the inverted model is close to the average profile of the two homogeneous sections. The thickness of the homogeneous layers seems to be a secondary factor to distort the inverted composed model, as seen in cases 2a and 2b. Strong variations of velocity are more important.

Fixed thickness, multi-layer inversion (mode 2)

Inversion tests with more layers (which require fixed thicknesses) also provide useful information on the structure. We now invert only for the S-wave velocities using five layers (four 0.5 km thick and one 1.0 km thick) with the same search parameter ranges as used with the real data. We also fixed the velocity of the half-space (basement), as in the previous synthetic tests because we want to concentrate on the effect of lateral variation in the sedimentary layers. An initial test was carried out (Figure 9) to confirm that our HGA procedure can find the best solution in the multi-layer inversion mode.

Using this un-smoothed multi-layer inversion, the composed data from the same inhomogeneous sections (1a-d, 2a-b and 3a-c) were inverted. The resulting models are shown in Figures 10–12. For small differences in the two homogeneous sections, cases 1am, 1bm (Figures 10a, b) and 2am, 2bm (Figure 11 a, b), the inverted models give the average velocities of the two sections, as in the previous inversion mode. For the cases 3am and 3bm (Figure 12), when both thickness and velocities are changed, the inverted models also show roughly the average S-wave profile.

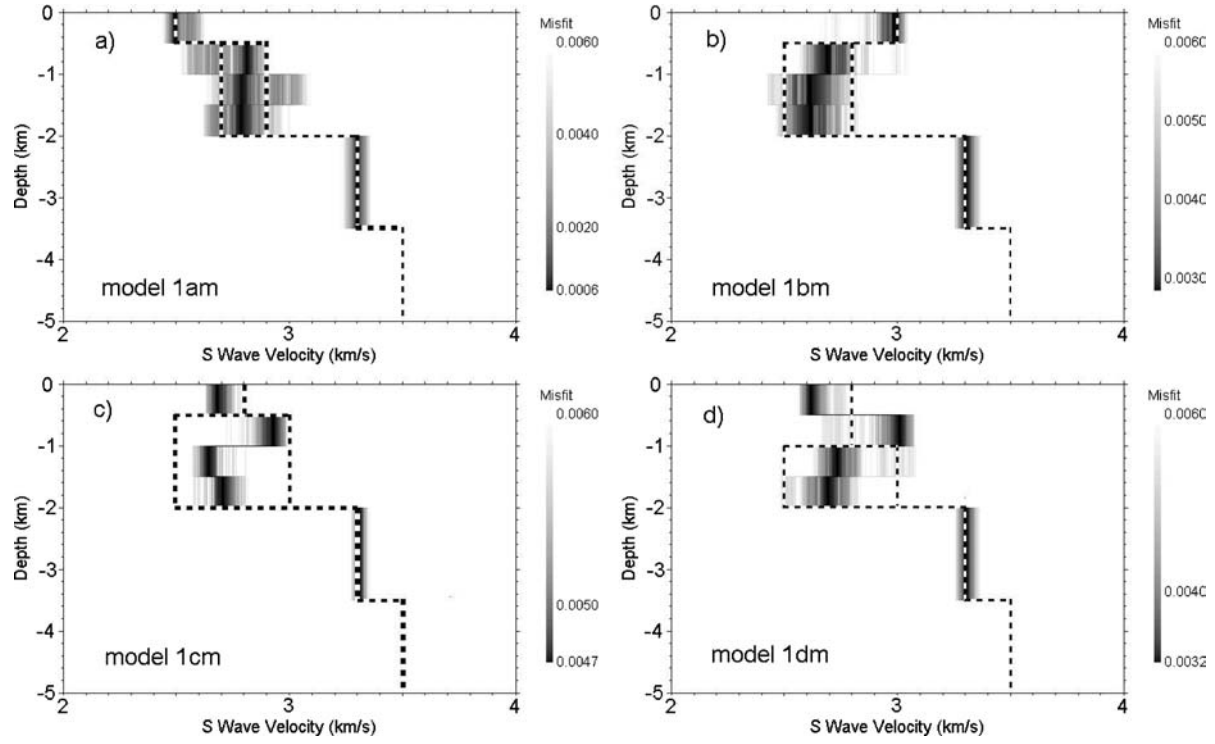

Figure 10. The good inverted models of group 1 (S velocity variation in the second layer) in the inversion mode 2.

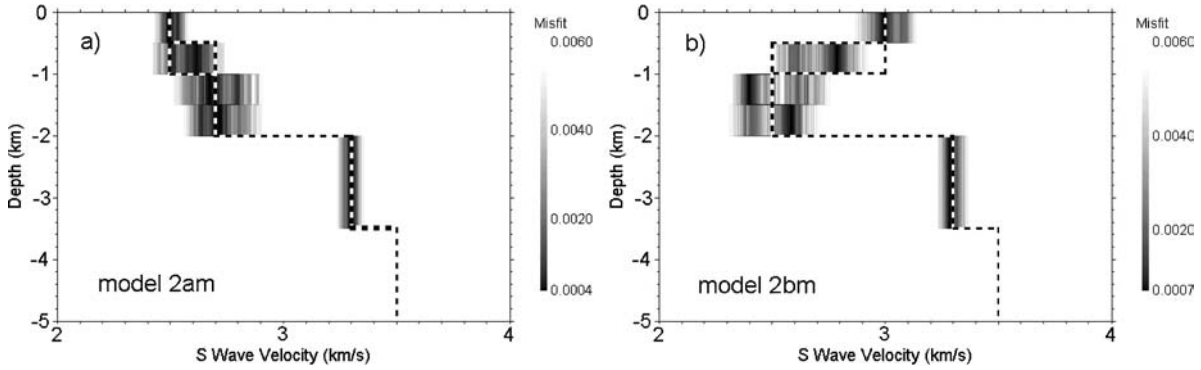

Figure 11. The good inverted models of group 2 (thickness variation in the first and second layers) in the inversion mode 2.

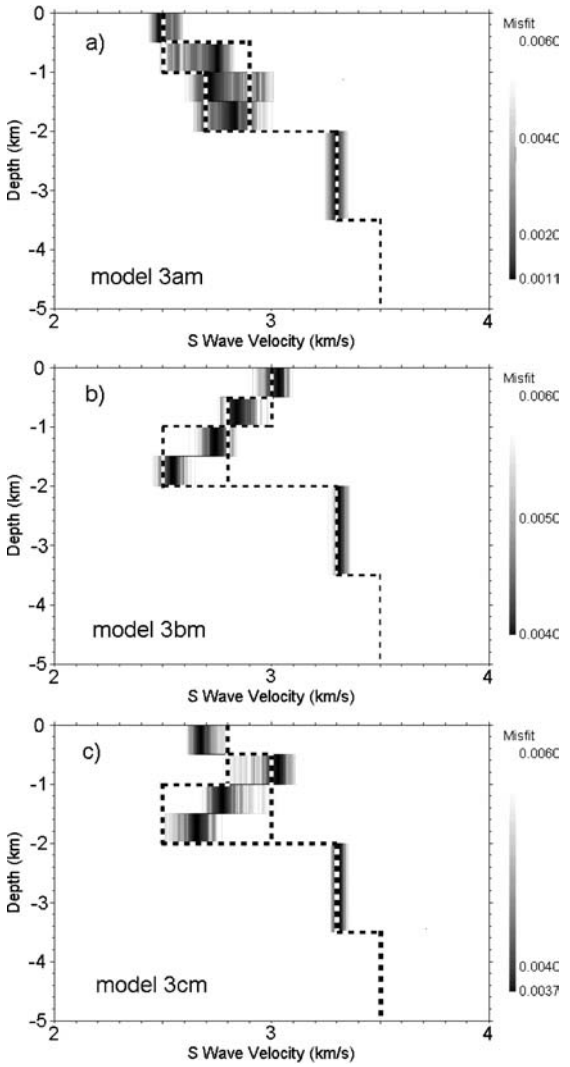

Figure 12. The good inverted models of group 3 (thickness and S velocity variation in the first and second layers) in the inversion mode 2.

When lateral variation is stronger (cases 1 cm, 1 dm and 3 cm), the inverted models show significant differences from the average profiles. In these cases, an artificial oscillation in the top two layers is observed. More importantly, however, is that the resulting inverted models are very different compared with the previous inversion mode 1 (Figures 6c, d and 8c). This implies that the "average" 1-D model, in the presence of strong lateral variations can be highly dependent on the model parameterization, and this must be taken into account when interpreting the inversion of observed data.

Fixed thickness, smoothed multi-layer inversion (mode 3)

Smoothness constraints can remove artificial oscillations in the S-wave velocity profile when only the general trend of the S-wave velocities is of interest. For the cases of small lateral variation (such as cases 1am, 1bm, 2am, 2bm, where the inverted models, in the unsmoothed inversion mode 2, are close to the average properties of the two homogeneous sections) smoothness constraint would not improve the inverted models any further. So we only analyze model 1dm (Figure 10d) which shows strong oscillation in the first layer. When smoothness constraints are used in the first four layers (Figure 13), the average trend of S-wave velocities is obtained.

Discussion and conclusion

Because no artificial errors were added to the synthetic data, the above tests show that some strange features or strong velocity oscillations in the inverted 1D models can arise from a dispersion curve which

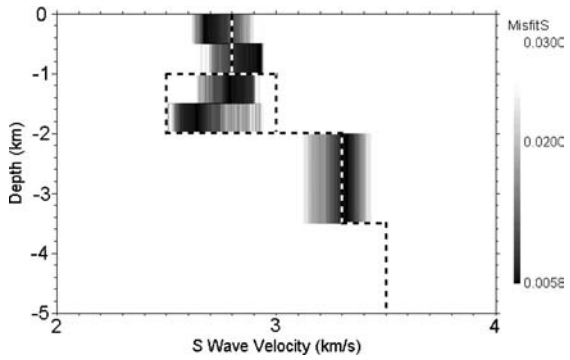

Figure 13. Inversion mode 3 with smoothness constraint in the shallow four layers down to 2 km only. The good inverted models in grayscale of misfitS ($Q_u + 0.007\,Q_{\text{smooth}}$) have smoothness <0.2 km/s. Synthetic data are from model 1dm in Figure 10d.

samples large lateral variation along the propagation path. In a different study, synthetic tests using long period observations of phase and group velocities to obtain lithospheric models for the Paraná Basin (An and Assumpção, 2005) also showed similar effects.

In real observations, the propagation path seldom covers a perfectly homogeneous structure, and the surface wave velocities will be affected by the horizontal heterogeneity as shown by Kennett and Yashizawa (2004) for refracted paths across the continent/ocean boundary. Our tests showed that the horizontal heterogeneity can also cause some uncertainties on the inverted path-average model even when the surface waves suffer no lateral refraction. The synthetic tests showed that inversion of surface wave dispersion can produce different models depending on the chosen parameterization for the strongly heterogeneous path, and analysis of these differences can provide some information on the propagation path. This suggests that one should carry out inversions with different model parameterizations (such as inversion modes 1 and 2) and compare the common features of the resulting models. If the results of different inversion modes are similar, they can represent an average structure along the propagation path. Otherwise if they are very different and the inverted models include large velocity oscillations between neighboring layers, it is possible that the propagation path has strong lateral variations. In this case, the inverted model may differ significantly from the average structure, and smoothness constraints will be necessary for an estimate of the general S-wave velocity trend.

The inversions of our real data (Figure 3) for both POPB and CANB show that, between 0.5 km and 2 km depth, the results of inversion mode 1 and 2 are different, and the un−smoothed multi-layer model (mode 2) includes strong velocity oscillation between neighboring layers. This effect is more obvious for POPB than CANB. The inverted S-wave velocity models of POPB show similar effects as the synthetic tests with strong lateral variation in Figures 10c, d and 12c. We believe these inversion tests indicate strong horizontal heterogeneity of S-wave velocity at least down to 2 km depth. The inverted un-smoothed models of CANB have fewer oscillations than those of POPB, meaning that the CANB path is probably less inhomogeneous than that of POPB, which is consistent with the available geological information (Figure 1c).

Inversion of group velocities (1–4.2 s) to study the shallow structure in the Paraná Basin, produced S-wave velocity profiles roughly consistent with the available geological and borehole information and showed that the low-velocity zone with pre-volcanic sediments can be studied with surface waves. However, the comparison of the resulting models using different inversion modes suggests strong lateral heterogeneity in the first few kilometers, which is consistent with the expected depth variations in the basin. Average basement depths were estimated at about 3.5 km and 3.2 km (for POPB and CANB paths, respectively), but synthetic tests show that lateral variation effects can induce errors of about 0.5 km. Basement velocities were higher for the CANB path compared with the POPB path, both in the S-wave/thickness inversion mode 1 and the fixed-layer inversion mode 2. It is possible that the lower half-space velocity in the POPB model is actually representing a transition zone to a higher velocity basement, whereas the CANB half-space is already sampling below this transition zone.

The two paths we used, although sampling different average thicknesses, resulted in models with the same vertical averaged S-wave velocity for the basin layer: 2.4–2.7 km/s for all models in the three inversion modes (Figure 3). This average S-wave velocity of about 2.6 km/s for the basin will be useful to help constrain deep crustal models obtained from long period teleseismic surface wave.

Acknowledgments

Work financed by grants 01/06066-6 and 00/07134-2 (FAPESP-Brazil). We thank Robert Herrmann and Arthur Snoke for discussions on various aspects of

surface wave processing. We also thank David M. Boore for good suggestions on this paper.

References

An, M. and Assumpção, M., 2001, Surface wave dispersion inversion using improved genetic algorithm (extended abstract). *7th International Congress of the Brazilian Geophysical Society*, Salvador, Brazil, October. CD-ROM.

An, M. and Assumpção, M., 2005, Crustal and upper mantle structure in intracratonic Paraná Basin, SE Brazil, from surface wave dispersion using genetic algorithm, *J. South Am. Earth Sci.*, accepted.

An, M. and Shi, Y., 1996, Dynamic genetic algorithms inversion of earthquake focal mechanism from P waves first motions (in Chinese), *Earthquake Research in China* **12**(4), 394–402.

Assumpção, M., Barbosa, J.R., Berrocal, J., Bassini, A., Veloso, J.A.V., Mârza, V., Huelsen, M. and Ribotta L.C., 1997, Seismicity patterns andfocal mechanisms in SE Brazil, *Rev. Bras. Geofísica* 15, 119–132.

Assumpção, M., James, D.E. and Snoke, J.A., 2002, Crustal thickness in SE Brazilian shield by receiver function analysis: Implications for isostatic compensation, *J. Geophys. Res.* **107**(B1), 10.1029/2001JB000422.

Boore, D.M. and Joyner, W.B., 1997, Site amplifications for generic rock sites, *Bull. Seismol. Soc. Amer.* **87**(2), 327–341.

Bhattacharya, S.N., 1983, Higher order accuracy in multiple filter technique, *Bull. Seismol. Soc. Amer.* **73**, 1395–1406.

CESP, 1991, Análise dos sismogramas da rede de Capivara (SP/PR), de 01/06 a 31/12/1990. Relatório, LEC-GE-10/91, Cia. Energetica de Sao Paulo – CESP, 107.

Chourak, M., Badal, J., Corchete, V. and Serón, F.J., 2001, A survey of the shallow structure beneath the Alboran Sea using Rg-waves and 3-D imaging, *Tectonophysics* **335**, 255–273.

Christensen, N.J. and Mooney, W.D., 1995, Seismic velocity structure and composition of continental crust: A global view, *J. Geophys. Res.* **100**(B6), 9761–9788.

DAEE, 1976, Estudo de águas subterrâneas, Regiões administrativas 7, 8, 9. Departamento de Água e Energia Elétrica, São Paulo, SP, Brazil.

DAEE, 1979, Estudo de águas subterrâneas, Regiões administrativas 10 e 11. Departamento de Água e Energia Elétrica, São Paulo, SP, Brazil.

Dziewonski, A., Bloch, S. and Landisman, M., 1969, A technique for analysis of transient seismic signals, *Bull. Seismol. Soc. Amer.* **59**(1), 427–444.

Herrin, E. and Goforth, T., 1977, Phase-matched filters: Application to the study of Rayleigh waves, *Bull. Seismol. Soc. Amer.* **67**, 1259–1275.

Herrmann, R.B., 1987, *Computer Programs in Seismology*. St. Louis University. St. Louis, MO.

Herrmann, R.B., 2001,*Computer Programs in Seismology – An Overview of Synthetic Seismogram Computation*. St. Louis University, St. Louis, MO.

Herrmann, R.B. and Ammon, J.C., 2002, *Computer Programs in Seismology – Surface Waves, Receiver Functions and Crustal Structure*. St. Louis University, St. Louis, MO.

Kennett, B.L.N. and Yoshizawa, K., 2002, A reappraisal of regional surface wave tomography, *Geophys. J. Int.* 150, 37–44.

Kocaoglu, A.H. and Long, L.T., 1993, Tomographic inversion of Rg wave group velocities for regional near-surface velocity structure, *J. Geophys. Res.* **98**, 6579–6587.

Levshin, A.L., Ritzwoller, M.H., Barmin, M.P., Ratnikova, L.I. and Padget, C.A., 1998, Automated surface wave analysis using phase-matched filters from dispersion maps. *Proceedings of the 20th Seismic Research Symposium on Monitoring a CTBT*, pp. 466–473.

Lomax, A. and Snieder, R., 1995, The contrast in upper mantle shear-wave velocity between the East European Platform and tectonic Europe obtained with genetic algorithm inversion of Rayleigh-wave group dispersion, *Geophys. J. Int.* **123**, 169–182.

Melfi, A.J., Piccirillo, E.M. and Nardy, A.J.R., 1988, Geological and magmatic aspects of the Paraná basin – An introduction, in Piccirillo, E.M. and Melfi, A.J. (eds.), *The Mesozoic Flood Volcanism of the Paraná Basin – Petrogenetic and Geophysical Aspects*, Instituto Astonômico e Geofísico – Universidade de São Paulo, pp. 1 – 13.

Schobbenhaus, C. and Bellizzia, A. (coord.), 2001, Geological Map of South America, 1:5000000. CGMW-CPRM-DNPM-UNESCO, Brasilia.

Shi, Y. and Jin, W., 1996, Genetic algorithm inversion of lithospheric structure from surface wave dispersion, *Chinese J. Geophys.* **39**(1), 101–111.

Snoke, J.A. and James, D.E., 1997, Lithospheric structure of the Chaco and Paraná Basins of South America from surface-wave inversion, *J. Geophys. Res.* **102**, 2939–2951.

Snoke, J.A. and Sambridge, M., 2002, Constraints on the S wave velocity structure in a continental shield from surface wave data: Comparing linearized least squares inversion and the direct search Neighbourhood Algorithm, *J. Geophys. Res.* 107, 10.1029/2001JB000498.

Stanley, W.D., Saad, A.R. and Ohofugi, W., 1985, Regional magnetotelluric surveys in hydrocarbon exploration, Paraná basin, Brazil, *The American Association of Petroleum Geologists Bulletin* **69**(3), 346–360.

Stokoe, K.H., II, and Nazarian, S., 1983, Effectiveness of ground improvement from spectral analysis of surface waves, in: *Proceedings of the Eighth European Conference on Soil Mechanics and Foundation Engineering*, Helsinki.

Stokoe, K.H., II, Rix, G.J. and Nazarian, S., 1989, *In situ* seismic testing with surface waves, in: *Proceedings of the Twelfth International Conference on Soil Mechanics and Foundation Engineering*, Rio de Janeiro, Brazil, **1**, pp. 330–334.

Yamanaka H. and Ishida H., 1996, Application of genetic algorithms to an inversion of surface wave dispersion data, *Bull. Seismol. Soc. Amer*. **86**(2), 436–444.

Zalán, P., Wolff, S., Conceição, J., Astolfi, M, Vieira, I., Appi, V., Zanotto, O. and Marques, A., 1988, *Tectonics and sedimentation of the Paraná basin. Seventh International Gondwana Symposium* (São Paulo, Brazil, July).

Zalán, P., Wolff, S., Conceição, J., Marques, A., Astolfi, M., Vieira, I., Appi, V. and Zanotto, O., 1990, Bacia do Paraná, in Raja Gabaglia, G. and Milani E. (eds.), *Origem e Evolução das Bacias Sedimentares,* Petrobrás, Brazil, pp. 135–168.

Zhang, K., Snoke, J.A., and James, D.E., 1998, Lithospheric structure of the eastern Paraná basin of central Brazil from surface-wave inversion: Comparing genetic algorithms and linearized least-squares inversion. IRIS Workshop (Santa Cruz, CA, July).